Applied Catalysis B: Environmental 248 (2019) 54–61

Contents lists available at ScienceDirect

Applied Catalysis B: Environmental

journal homepage: www.elsevier.com/locate/apcatb

Assessment of different iron species as activators of $S_2O_8^{2-}$ and HSO_5- for inactivation of wild bacteria strains

Jorge Rodríguez-Chueca[a,*], Sonia Guerra-Rodríguez[a], Julia M. Raez[b], María-José López-Muñoz[b], Encarnación Rodríguez[a]

[a] Department of Industrial Chemical & Environmental Engineering, Escuela Técnica Superior de Ingenieros Industriales, Universidad Politécnica de Madrid, Calle José Gutiérrez Abascal 2, 28006, Madrid, Spain
[b] Department of Chemical and Environmental Technology, Universidad Rey Juan Carlos, Calle Tulipán s/n, 28933, Móstoles, Spain

ARTICLE INFO

Keywords:
Wastewater disinfection
Escherichia coli
Enterococcus sp.
Persulfate (PS) vs. Peroxymonosulfate (PMS)
Sulfate radicals
Iron species

ABSTRACT

This work assesses the potential activation of peroxymonosulfate (PMS, HSO_5^-) and persulfate (PS, $S_2O_8^{2-}$) by different homogeneous iron species, $FeSO_4$ and Fe(III)-citrate and heterogeneous Fe_2O_3 and nano zero valent iron particles (nZVI), to generate sulfate radicals for inactivation of wild bacteria strains (*Escherichia coli* and *Enterococcus sp.*) spiked in simulated wastewater effluents. The effectiveness of each iron source as activator was studied in combination with UV-A radiation at natural pH of water (≈ 7.2) using millimolar doses of oxidants (0.5 mM) at different oxidant:iron molar ratio (1:1 and 1:2). In all cases, the addition of iron enhanced the efficiency of the treatments compared to those carried out without it (PMS/UV-A and PS/UV-A); however, significant differences were evidenced depending on the type of bacteria, oxidant and iron specie. For instance, *Escherichia coli* was reduced (5-log) below the limit of detection (1 CFU/mL) within 2–15 min by activation of PMS and PS with all the iron species evaluated By contrast, under analogous operating conditions the efficiency was notably lower for *Enterococcus sp.* In this case, it is worth mentioning the notable efficiency through the use of Fe(III)-citrate, which allowed to attained a 3.50-log removal of *Enterococcus sp.* after 90 min, in contrast to the low reduction (1.8-log) attained with $FeSO_4$. On the other hand, heterogeneous iron species showed an efficiency for bacteria inactivation comparable in most cases to that of homogeneous iron sources. Taking into consideration the potential advantages of heterogeneous catalysts, as for example the recovery and reuse of the catalyst thus reducing the operating costs, the obtained results are encouraging. For instance, *E.coli* population was removed below the detection limit (5-log) in less than 5 min with both Fe_2O_3 and ZVI, whereas a 2-log decrease of *Enterococcus sp.* was attained after 90 min of treatment, even without PMS. Finally, it was assessed the recovery and re-use of ZVI particles. According to X-Ray Diffraction (XRD) and Transmission Electron Microscopy (TEM) analysis, the reaction conditions induced a progressive fading of the core-shell structure of nZVI particles, with a decrease of the efficiency for bacteria inactivation in subsequent uses. As an example, *E.coli* is reduced in 5-log in 15 min in the first use, and 4.70-log in 90 min with the third use of ZVI.

1. Introduction

The hydric stress occurs when the available water cannot fulfil the demand required for basic domestic, agricultural and industrial uses. It is expected that more than 3.5 billion of people could experience water scarcity by 2020, being this situation extremely serious in the Mediterranean countries, the Middle East, Central and Southeast Asia, among others [1]. For that reason, the regeneration and reuse of treated urban wastewater is an interesting option for increasing the available water supplies [2].

The sulfate radical based-Advanced Oxidation Processes (SR-AOPs) have emerged as a feasible technology to remove organic pollutants [3–7], with a high potential to be used as an alternative to conventional disinfection agents [8–11]. SR-AOPs promote the generation of sulfate radicals ($SO_4^{-\bullet}$) through the activation of peroxymonosulfate (PMS, HSO_5^-) or persulfate (PS, $S_2O_8^{2-}$), via photolysis with UV radiation (Eqs. (1) and (2)) and/or catalysis with transition metals such as iron (Eqs. (3)–(5)), among other activation methods [12]. Based on the activation methods, the redox potential of sulfate radical is equal or even higher (2.5 – 3.1. V) [13] than hydroxyl radicals (2.8 V) [14].

The photolytic activation of PMS and PS generates sulfate radicals by fission of the O—O bond by energy input of UV (Eqs. (1) and (2))

* Corresponding author.
E-mail address: jorge.rodriguez.chueca@upm.es (J. Rodríguez-Chueca).

https://doi.org/10.1016/j.apcatb.2019.02.003
Received 5 October 2018; Received in revised form 15 January 2019; Accepted 3 February 2019
Available online 05 February 2019
0926-3373/

[12]. In addition, it must be highlighted the simultaneous generation of hydroxyl radicals in the photolytic activation of PMS.

$$HSO_5^- \xrightarrow{h\nu} SO_4^{\bullet -} + HO^{\bullet} \quad (1)$$

$$S_2O_8^{2-} \xrightarrow{h\nu} 2SO_4^{\bullet -} \quad (2)$$

Herrmann (2007) [15] reported the quantum yields for photolysis of PS and PMS. The maximum quantum yield (φ = 1.4) was obtained for PS in the range of range of 248–253.7 nm. While, the value for PMS photolysis is lower (φ = 0.12; λ = 248 nm). However, although Herrmann (2007) [15] reported that the quantum yield decreases with the increase of the wavelength, some authors have also reported the activation of PMS and PS in the range of UV-A [8–10,12].

The Fe(II)-catalytic activation of PMS is regulated by two main reactions (Eqs. 3 and 4); Fe(II) acts as electron acceptor prompting the rupture of the HO bond in the PMS structure, while Fe(III) formed reacts with PMS generating the sulfur pentoxide radical. This radical has a redox potential (E° = 1.1 V) lower than hydroxyl and sulfate radicals, but high enough to cause damages in bacteria. This catalytic cycle of iron is not observed when coupled with PS so after oxidation of Fe(II) (Eq. (5)) there is no PS-mediated reduction of Fe(III).

$$HSO_5^- + Fe^{2+} \rightarrow SO_4^{\bullet -} + Fe^{3+} + OH^- \quad k = 3.0 \cdot 10^4 M^{-1} \cdot s^{-1} \quad (3)$$

$$HSO_5^- + Fe^{3+} \rightarrow Fe^{2+} + SO_5^{\bullet -} + H^+ \quad k = notfound \quad (4)$$

$$S_2O_8^{2-} + Fe^{2+} \rightarrow Fe^{3+} + SO_4^{\bullet -} + SO_4^{2-} \quad k = 12\text{–}27 M^{-1} \cdot s^{-1} \quad (5)$$

Several authors have studied the efficiency of different metals to promote the activation of PMS and PS [12,16–18]. There is a wide agreement that cobalt and iron are the most recommended species to activate PMS [17–20], while silver shows the best efficiency for PS [17]. Withal, although maybe less effective, the use of iron should be preferable because of its low toxicity for humans and environment.

According to the Gram staining technique, bacteria are divided in two main groups. Gram-negative bacteria have a cytoplasmic membrane, a thin peptidoglycan layer and an outer membrane containing lipopolysaccharides. Meanwhile, Gram-positive bacteria have only a cytoplasmic lipid membrane and the peptidoglycan layer is thicker than that of Gram-negative bacteria. Because of these structural differences, Gram-positive bacteria as *Enterococcus sp.* are usually more resistant to treatments than Gram-negative bacteria as *Escherichia coli* [21]. For this reason, the use of Enterococcus sp. as indicator is preferred instead of E.coli.

The aim of this study was to comparatively study the PMS and PS activation by different iron species. Four iron activators were tested: two in homogeneous mode, $FeSO_4$ and Fe(III)-citrate, and two in heterogeneous phase (Fe_2O_3 and nano zero valent iron (nZVI)). These SR-AOPs treatments were evaluated on the inactivation of *E.coli* and *Enterococcus sp.* wild strains spiked in simulated wastewater samples. All the treatments were applied in combination with UV-A radiation with the objective of increasing the bacterial inactivation kinetics. The concentration of the different reactants was optimized using millimolar doses, in the context of their potential application as tertiary treatment to regenerate wastewater. Moreover, the recovery and reuse of nZVI was studied in order to ascertain whether this heterogeneous catalyst might be used in subsequent uses without a loss of efficiency.

2. Material and methods

2.1. Isolation of wild strains of Escherichia coli and Enterococcus sp

Escherichia coli and *Enterococcus sp.* wild strains were selected in effluent samples collected from a wastewater treatment plant (WWTP) located in Madrid (Spain). They were isolated by cultivation on selective culture medium (MacConkey and Slanetz&Bartley agar (Scharlau) for *E.coli* and *Enterococcus sp.* respectively) and incubation at 37 °C during 24 h for *E.coli* and 48 h for *Enterococcus sp.* After that, a single colony from each plate was inoculated into 20 mL sterile Luria Bertani broth (Scharlau), and incubated for 20 h at 37 °C. After the incubation, bacterial suspensions were diluted in the reactor to an initial concentration of 10^6 CFU/mL.

2.2. Aqueous matrix preparation

Simulated wastewater was used as a model matrix for the assessment of treatments efficiency, also guaranteeing the reproducibility of the experimental conditions in the different runs. The composition of simulated effluent wastewater was: meat peptone (Scharlau; 160 mg/L), meat extract (Scharlau; 110 mg/L), urea (Scharlau; $CO(NH_2)_2$; 30 mg/L), NaCl (Scharlau; 7 mg/L), $CaCl_2{\cdot}2H_2O$ (Scharlau; 4 mg/L), $MgSO_4{\cdot}7H_2O$ (Scharlau; 2 mg/L), K_2HPO_4 (Scharlau; 28 mg/L) and deionized water [22]. The physico-chemical characteristics of simulated water (pH ≈ 7.2; turbidity = 2 ± 0.5; Chemical Oxygen Demand = 19 ± 4 mg/L) were similar to real treated wastewater.

2.3. Chemical and reagents

Treatments were performed using different dosages (0.01–1 mM) of potassium peroxymonosulfate ($2KHSO_5{\cdot}KHSO_4{\cdot}K_2SO_4$, PMS, Merck) and sodium persulfate ($Na_2S_2O_8$, PS, Scharlau). As iron sources iron (II) sulfate heptahydrate ($FeSO_4{\cdot}7H_2O$, Panreac), iron (III) oxide (Fe_2O_3, Scharlau), iron (III) citrate ($C_6H_5FeO_7$; ACROS Organics) and nano zero-valent Fe (nZVI) were used in different molar ratio (oxidant:iron; 1:1-1:2) and different load for nZVI (50–100 mg/L).

2.4. Synthesis of nZVI

nZVI particles used in this study were synthesized by reduction and precipitation of a dissolved iron salt in absence of oxygen modifying a method previously reported [23]. First, a solution of $FeSO_4{\cdot}7H_2O$ (> 99%, Aldrich) 0.4 M in ultrapure water and ethanol (> 99%, Scharlau) (70:30 v/v) was prepared and sonicated until the complete dissolution of the iron salt. The chemical coprecipitation of iron was performed by increasing the value of pH until 6.8 with NaOH (> 98%, Aldrich) 3.8 M. In order to reduce the ferrous ions to Fe(0) an excess of $NaBH_4$ was added into the mixture. The solution was well homogenized and washed with pure water and ethanol. Finally, the metallic iron was recovered by filtration and dried under vacuum prior characterization.

2.5. Pre- and post- treatment characterization of nZVI

The crystalline structure of nZVI was analyzed by X-Ray Diffraction (Philips X-PERT MPD diffractometer) with CuK_α radiation. The morphology, size particle and elemental composition of the samples was determined by Transmission Electron Microscopy (TEM) using a JEOL JEM 2100 microscope with an accelerating voltage of 200 kV, equipped with X-Ray Energy Dispersive Spectroscopy (XEDS) and Low-Energy Electron Diffraction (LEED).

2.6. Experimental setup

The experiments were performed in an annular batch lab—scale reactor with recirculation, with a total volume of 1 L and illuminated volume of 0.252 L (25.2% of total water sample). Experiments were performed at natural pH of simulated wastewater samples (≈ 7.2), because previous research [18] proved the low dependence of PMS to pH. It is worthy to remark this fact, because the possibility to treat wastewater at neutral pH means a reduction in the operating costs.

Illumination of the reactor was provided by a black light lamp (Philips TL 6 W; 365 nm) located in the axis of the annular reactor. According to the illuminated volume (0.252 L) and the flow rate (6.4 L/

min), the UV-A contact time was 2.36 s. As experiments lasted 90 min, therefore the water sample was illuminated a total time of 22.7 min.

2.7. Microbial methods

The culture and enumeration of the microorganisms was carried out by the spread plate method (Standard Method 9215C; [24]) through a serial 10-fold dilution in sterile saline solution (NaCl 0.9%). Samples were plated on MacConkey Agar (Scharlau; Spain) for *E.coli* and Slanetz &Bartley agar (Scharlau; Spain) for *Enterococcus sp.* Colonies of both bacteria were counted after incubation at 37 °C (24 h for *E.coli* and 48 h for *Enterococcus sp.*). The detection limit (DL) of this experimental procedure was 1 CFU/mL.

The enumeration of colonies was expressed as CFU/mL (colony-forming units). These concentrations were transformed to log10 and the removal of bacteria, D = Log (N_t/N_0), was calculated from the initial bacteria concentration (N_0) and the remaining bacteria population at t time (N_t).

3. Results and discussion

The ability of PMS and PS to damage bacteria is strongly dependent on the concentration of both oxidants. Previous research [25] showed that PMS concentrations higher than 0.1 mM lead to some bacteria reduction after 4 h of contact time in darkness. This value was taken as reference to optimize the treatments.

3.1. UV-A photolytic activation of PMS and PS

In a first approach it was tested the activation of PMS and PS by UV-A radiation, using different oxidant dosages (0.01–1 mM). Fig. 1 shows the results for inactivation of *E.coli* and *Enterococcus sp.* attained with each oxidant. In both cases, their combination with UV-A improved the performance of UV-A alone, which shows a negligible reduction of bacterial population. As observed, PMS induced a higher inactivation of bacteria than PS. For instance, the limit of detection (1 CFU/mL; 5-log) for *E.coli* was reached after 30 min of reaction upon addition of 1 mM of PMS, while a reduction of 2-log was observed after 90 min using the same dosage of PS (Fig. 1A). By contrast in accordance with previous reports [21], a strong tolerance to the treatments was observed in the case of *Enterococcus sp.*, requiring 90 min to reach the detection limit (1 CFU/mL; 6-log).

The different behavior of both oxidants is easily understandable considering the Eqs. (1) and (2). The photolysis of the PMS molecule generates not only a sulfate radical but also a hydroxyl one, while in the case of PS, two sulfate radicals are generated, which makes the difference. Sun et al. [26] suggest that because of the negative charge of sulfate radicals, it exists an electrostatic repulsion with the surface of bacteria, also negatively charged. This drawback is overcome with ·HO radicals, which can approach the bacteria surface more easily. For this reason, the additional generation of hydroxyl radicals from PMS increased the inactivation efficiency.

3.2. Homogeneous iron-mediated activation of PMS and PS

The bacteria inactivation by catalytic activation of PMS and PS (0.5 mM) was studied using $FeSO_4$ and Fe(III)-citrate in different oxidant:Fe molar ratios (1:1 and 1:2).

The coupling of PMS and PS with Fe(II) has been widely reported by other authors as an efficient way to increase the microbial inactivation kinetics [8–11]. Fig. 2 shows clearly the improvement in the inactivation kinetics compared to those treatments without Fe(II). This enhancement takes place over both bacteria, *E.coli* and *Enterococcus sp.*, however, it is notably higher for *E.coli*, for which total inactivation is observed after 2 min of reaction (oxidant:iron molar ratio 1:2). This fast inactivation can be ascribed to the continuous generation of oxidative

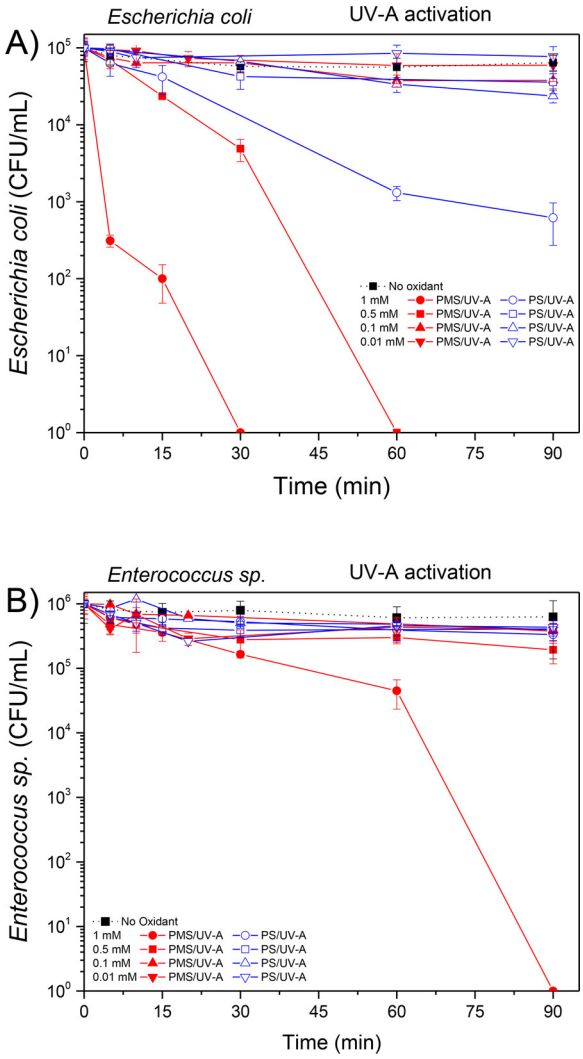

Fig. 1. Photolytic activation of PMS and PS by UV-A radiation for A) *Escherichia coli* and B) *Enterococcus sp.* inactivation.

species (sulfate, hydroxyl and sulfur pentoxide radicals; Eqs. (3)–(5)). In the case of PMS, iron has a catalytic cycle in which Fe(II) is continuously regenerated. Nevertheless, there is no PS-mediated reduction of Fe(III), being necessary the presence of radiation to promote the reduction to Fe(II) following Eq. (6) [27,28]:

$$Fe(OH)^{2+} \xrightarrow{h\nu} Fe^{2+} + HO^{\bullet} \quad \varphi = 0.017\,(\lambda = 360\,nm) \tag{6}$$

Enterococcus sp. reduction was much lower than the observed for *E.coli*. Even though the presence of Fe(II) increased the removal achieved without it, the observed trend is a rapid reduction in the first five minutes of reaction (1-log) followed by a stabilization of the population until the end of the treatment. Although further research is needed, it is suggested that the higher resistance of *Enterococcus sp.* to treatments compared to *E.coli* is a consequence of the structural differences in the cell membrane of Gram-positive (*Enterococcus sp.*) and Gram-negative (*E.coli*) bacteria [21]. As a matter of fact, some authors have reported the tolerance of *Enterococcus sp.* to disinfection treatments as chlorination [29]. In addition, the higher resistance of *Enterococcus sp.* to treatments and their longer survival compared to coliforms and *E.coli* in water environment are some of the reasons why it is strongly recommended their use as faecal pollution indicator [21,30–33]. In general terms, these results agree with those reported previously by Rodríguez-Chueca et al. [8,9,25] using different operating conditions.

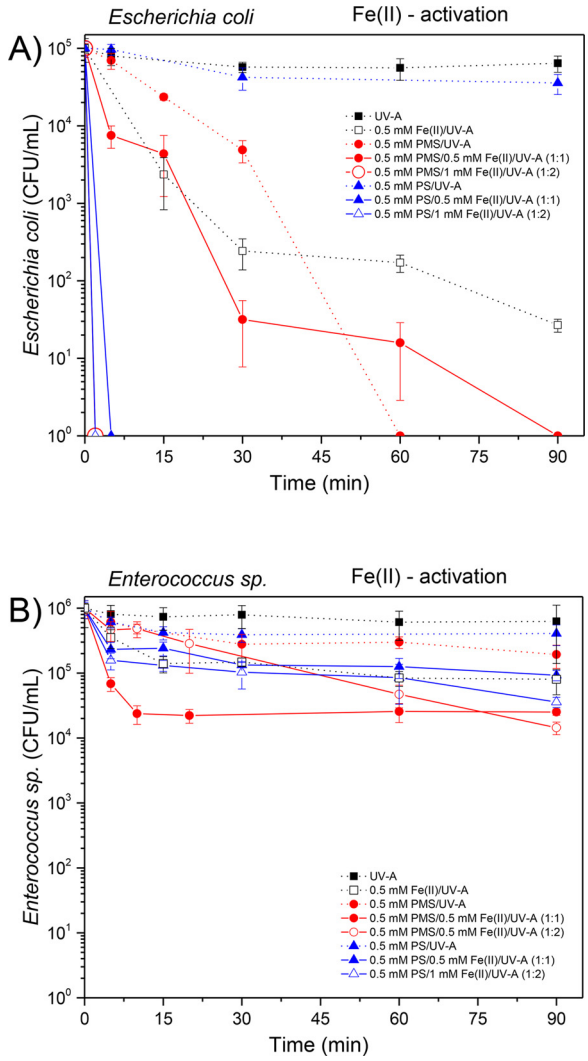

Fig. 2. Fe(II) catalytic activation of PMS and PS coupled with UV-A radiation for A) *Escherichia coli* and B) *Enterococcus sp.* inactivation.

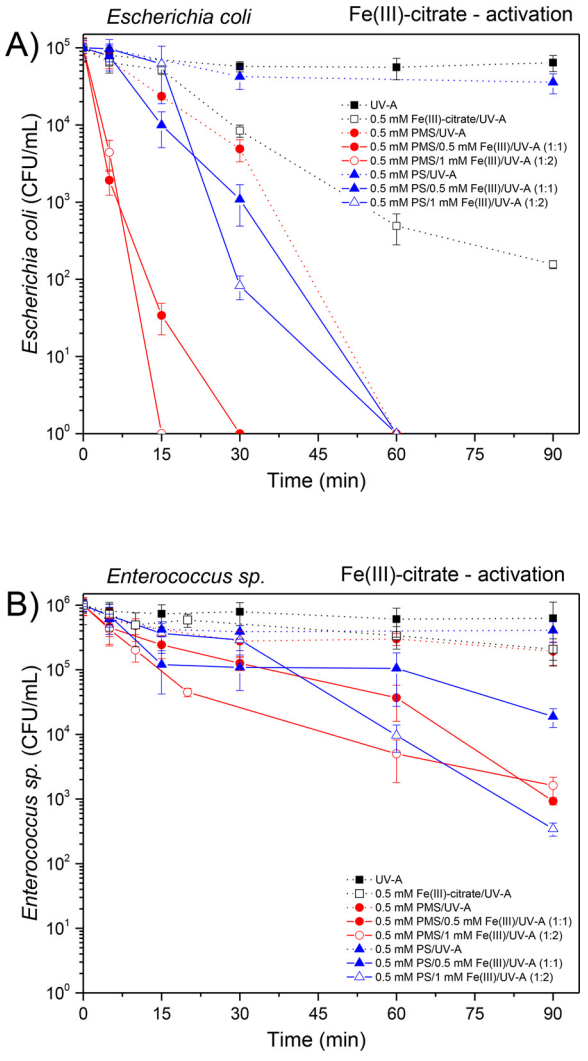

Fig. 3. Fe(III)-citrate catalytic activation of PMS and PS coupled with UV-A radiation for A) *Escherichia coli* and B) *Enterococcus sp.* inactivation.

Photochemistry of Fe(III)-carboxylate complexes as Fe(III)-citrate, is of interest for environmental applications among which oxidative processing of wastewater [34–37]. The literature on the application of citrate in chelating Fe(II) or Fe(III) to activate PMS or PS is limited [38–40]. Fig. 3 shows the results obtained by coupling Fe(III)-citrate with PMS and PS under UV−A radiation. Similarly to previous experiments the presence of Fe(III)-citrate enhances the bacteria inactivation kinetics in comparison to those treatments without iron, so that the complete inactivation of *E.coli* is attained with PMS and PS after 15 and 60 min, respectively (oxidant:Fe(III) molar ratio equal to 1:2). Although these are very good results, the comparison with those obtained using Fe(II) (Fig. 2) evidences a decrease in the efficiency to inactivate *E.coli*. This is particularly significant for PS as in this case, the time required to attain a 5-log reduction of *E.coli* increases from 2 min to 60 min with Fe (II) and Fe(III)-citrate, respectively.

The plausible explanation for this slight deceleration is that the reaction between PMS and Fe(III) only generates sulfur pentoxide radical but not sulfate and/or hydroxyl radicals (Eq. (4)). As above explained, the sulfur pentoxide radical has an oxidation potential (E^o = 1.1 V) able to cause damages in cells, however, it is lower than sulfate radicals (E^o = 2.5–3.1 V) decreasing the kinetics rate. In the case of PS, this oxidant does not react with Fe(III), therefore until Fe(III) is not photo-reduced to Fe(II) through Eq. (6), it does not start the generation of sulfate and hydroxyl radicals as consequence of reaction with PS.

Nevertheless, the behavior seems to be different for *Enterococcus sp.* because of the kinetics are faster with Fe(III)-citrate, but actually the mechanisms is the same as for *E.coli*. In this case, it can be proposed that as the removal of *Enterococcus sp.* is too slow under both operating conditions, it gives time for the appearance of new reactions increasing the generation of oxidizing radicals, helping to the global reduction of *Enterococcus sp.* These reactions would not be appreciable in the case of *E.coli* because of the much faster removal of these bacteria. As observed in Fig. 3B, the maximum *Enterococcus sp.* removal was around 3.50-log after 90 min, with both PMS and PS, respectively (oxidant:Fe(III) molar ratio equal to 1:2). It has been reported that the photolysis of Fe(III)-citrate generates hydrogen peroxide (H_2O_2) and superoxide radicals ($O_2^{\bullet -}$) (Eqs. (7)–(11)) [41]. Accordingly, H_2O_2 could promote a photo-Fenton reaction with Fe(II) present in water from photolysis of Fe(III)-citrate, thus generating hydroxyl radicals (Eq. (12)) [41].

$$Fe(III) - Cit \xrightarrow{h\nu} Fe(II) + Cit^{\bullet} \quad (7)$$

$$Cit^{\bullet} \rightarrow HO^{\bullet}CR_2 + CO_2 \quad (8)$$

$$HO^{\bullet}CR_2 + Fe(III) \longrightarrow R_2CO + H^+ + Fe(II) \quad (9)$$

$$HO^{\bullet}CR_2 + O_2 \longrightarrow R_2CO + H^+ + O_2^{\bullet -} \quad (10)$$

$$2H^+ + 2O_2^{\bullet -} \rightarrow H_2O_2 + O_2 \quad (11)$$

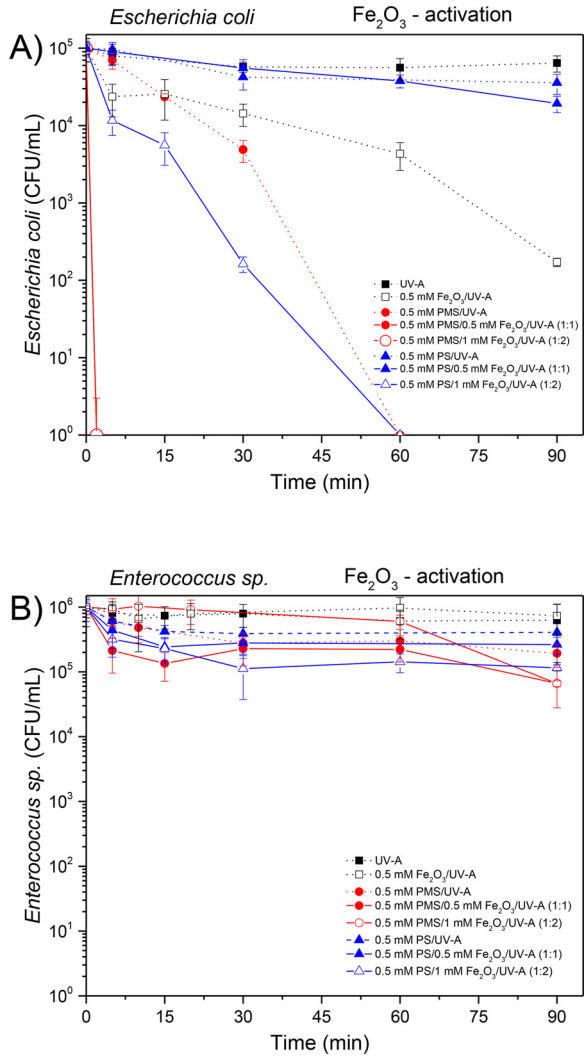

Fig. 4. Fe_2O_3 catalytic activation of PMS and PS coupled with UV-A radiation for A) *Escherichia coli* and B) *Enterococcus sp.* inactivation.

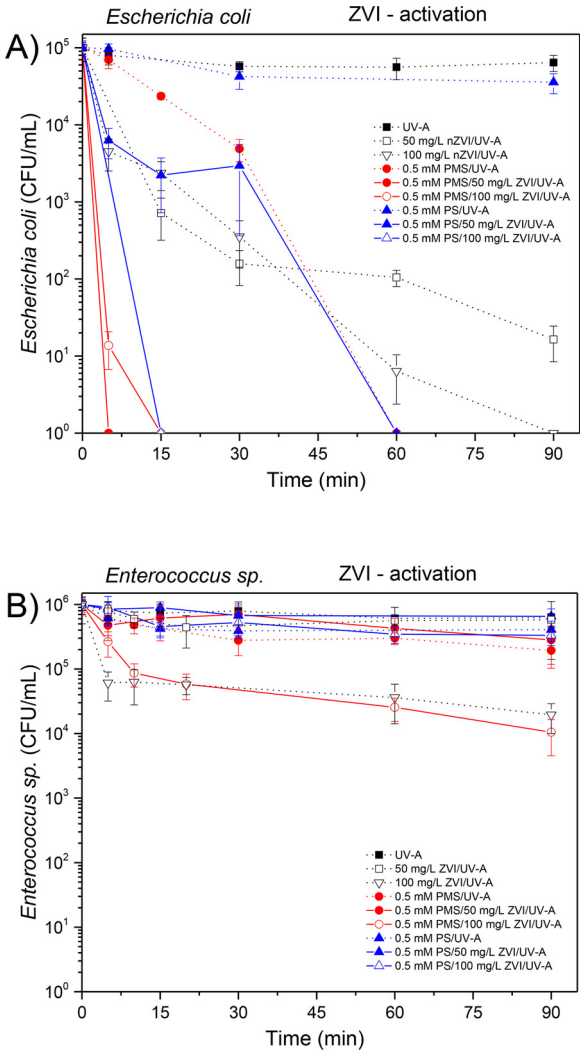

Fig. 5. nZVI catalytic activation of PMS and PS coupled with UV-A radiation for A) *Escherichia coli* and B) *Enterococcus sp.* inactivation.

$$H_2O_2 + Fe(II) \rightarrow Fe(III) + HO^{\bullet} + HO^{-} \quad (12)$$

3.3. Heterogeneous iron-mediated activation of PMS and PS

Heterogeneous iron mediated activation of PMS and PS might reduce the operating costs of the treatments, because it may be possible to recover and reuse the iron catalyst. In this context, two iron sources were evaluated with the same operating conditions above tested.

Fig. 4 shows the results for bacteria inactivation obtained with Fe_2O_3. As observed, the coupling of Fe_2O_3 with PMS allowed to reach the total inactivation of *E.coli* in a very short reaction time (2 min), even with the lower oxidant:Fe molar ratio, *i.e.* (1:1). By contrast, 60 min were required to reach the detection limit when Fe_2O_3 was combined with PS in a molar ratio of 1:2. Marjanovic et al. [10] reported the study of different iron oxides to activate PS under simulated solar radiation. In these conditions, they proved that Fe_2O_3 promoted a worse enhancement than $FeSO_4$ as Fe(II) activator in homogeneous form, reaching the total inactivation of *E.coli* K12 after 100 (Maghemite), 120 min (Hematite), and 60 min (Fe(II)). Ghanbari and Moradi [42] attributed the low kinetics in the activation with metal transition oxides to mass transfer limitations occurring in heterogeneous systems. In addition, the presence of Fe^{3+} (Eqs. (3)–(5)) on the surface of the oxide slows down the activation kinetics of PMS, while the activation of PS is not possible with Fe^{3+}, and it is required a photo-reduction to Fe(II) according to Eq. (6). In the case of *Enterococcus sp.*, similarly to the results obtained with dissolved Fe(II) in the homogeneous reaction, the application of iron oxide was not effective.

Finally, it was tested the efficiency of nZVI. The use of nZVI has been successfully reported for Fenton reactions [43–45] and, recently, in the activation of PMS and PS for the removal of organic compounds [46–48]. Nevertheless, from the best of our knowledge, this is the first time that is applied on bacterial inactivation. The treatments were applied with a catalyst load of 50 and 100 mg/L following previous results on removal of arsenic from water. Fig. 5 shows the results obtained for the inactivation of *E.coli* and *Enterococcus sp.*

As observed in the Fig. 5A, the coupling of nZVI with PMS increased notably the efficiency of *E.coli* removal if compared with photolysis of PMS, reaching a 5-log inactivation of bacteria after 5 min of contact time (50 mg/L of nZVI). A higher amount of nZVI (100 mg/L) did not enhance the efficiency, with similar kinetics. The results were also successful in the case of PS, but in this case, the increase of the catalyst load was necessary to increase the *E.coli* removal efficiency, requiring a final contact time of 15 min. It is important to highlight the high efficiency of the catalyst combined with UV−A in absence of oxidants. As observed in Fig. 5, there is a drop on bacteria population higher than 3-log after 30 min. This fact might mean a high leaching of iron. Alizadeh et al. [49] suggested that UV radiation could improve the nZVI solubility, increasing the microbial inactivation efficiency. On the other

hand, Morgada et al. [50] reported the hypothesis of FeO_x production from Fe° in presence of dissolved oxygen in water. This FeO_x together with UV radiation might produce Reactive Oxygen Species (ROS) according to the Eqs. (13)–(16), increasing the disinfection efficiency.

$$FeO_X + h\nu \rightarrow e_{cb}^- + h_{vb}^+ \quad (13)$$

$$HO^-(H_2O) + h_{vb}^+ \rightarrow HO^\circ(+H^+) \quad (14)$$

$$O_2 + e_{cb}^-(+H^+) \rightarrow O_2^-(HO_2^\circ) \quad (15)$$

$$O_2 + e_{cb}^- + H_2O_2 \rightarrow HO^\circ + HO^- \quad (16)$$

Yousefzadeh et al. [51] proved the efficiency of nZVI/UV radiation for inactivation of *Bacillus subtilis* spores. They reached a disinfection until 4-log after 60 min with 491 mg/L of nZVI. These results could not be compared with those reported herein for *E.coli*, because of the significant differences in resistance to treatments between both microorganisms [8,9].However, if compared with *Enterococcus sp.* (higher resistance than *E.coli*), it is also observed a large difference with the nZVI/UV inactivation efficiency reported by Yousefzadeh et al [51]. As shown in Fig. 5B, a maximum removal of *Enterococcus sp.* of 1.71-log was attained after 90 min with 100 mg nZVI/L. Results that can be explained by the higher loading of catalyst used by Yousefzadeh et al [51]. Besides, for *Enterococcus sp.* the addition of oxidants did not improve the bacteria removal efficiency, thus indicating that the bacteria removal is consequence of the presence of nZVI, not because of sulfate radicals.

Finally, it was tested the recovery and reuse of the catalyst. With this aim, the catalyst was removed from the water medium with the help of a neodymium magnet, and it was dried at 40 °C during 24 h. Fig. 6 shows the disinfection results after 3 uses of the nZVI (100 mg/L) combined with 0.5 mM of PMS. As observed, there is a gradual loss of efficiency after the consecutive uses. For *E.coli*, the time required to attain a 5-log inactivation increased from 15 min in the first use to 60 min in the second use. In the case of *Enterococcus sp.* the removal attained after 90 min decreased from 2-log in the first use to 0.66-log in the second use. In the third use of nZVI the efficiency of the treatment was also decreased, although in less extent. This loss of efficiency is a direct consequence of the iron leaching, because of the oxidation of nZVI in water. The action of oxidants such as PMS and PS favor this oxidation and the leaching. The pre- and post- characterization of nZVI confirmed this fact. Fig. 7 shows the XRD diffractograms of fresh and recovered nZVI after 1, 2 and 3 consecutives reactions. The peak at 2θ of 44.7° associated to α-Fe indicated that nZVI particles were mainly

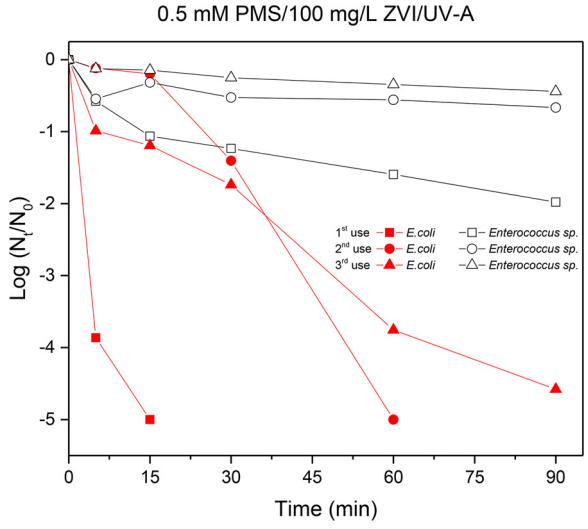

Fig. 6. Efficiency of nZVI coupled with PMSUV-A on the removal of *Escherichia coli* and *Enterococcus sp.* after consecutive uses.

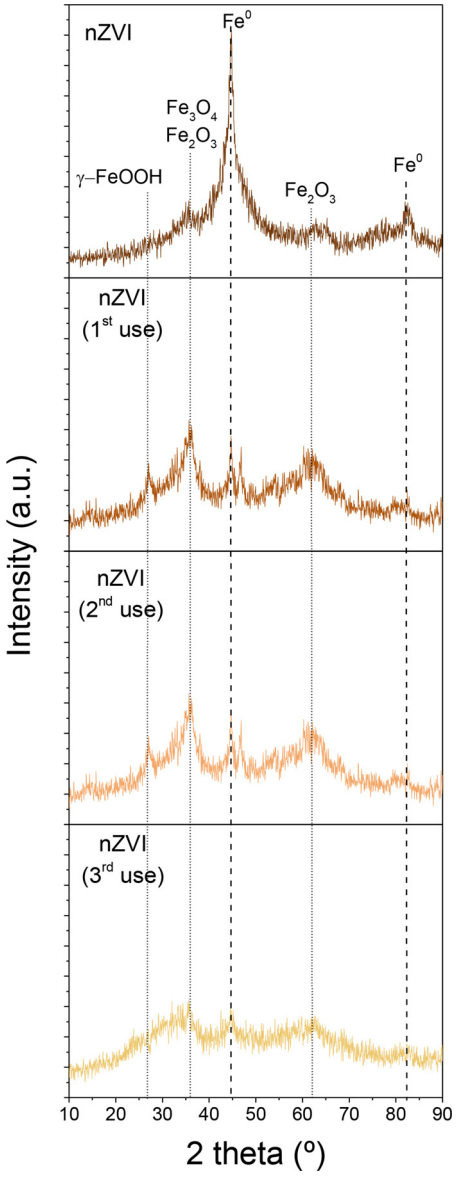

Fig. 7. XRD spectra of fresh nZVI and recovered after 1, 2 and 3 reactions.

composed by Fe(0). This peak was also observed in the diffractograms of the iron material recovered after the consecutive reactions, however, the signal becomes progressively weaker thus indicating the conversion of metallic iron into other species. Indeed, concomitantly to the fading of Fe(0) signal, different peaks associated to lepidocrocite (γ-FeOOH), magnetite (Fe_3O_4) or /and maghemite (Fe_2O_3) [52] were detected, revealing the progressive corrosion of nZVI in the oxygenated aqueous medium.

On the other hand, Fig. 8 shows evolution of the morphology of the nZVI material after being used in 3 consecutive reactions. Fresh nZVI material is comprised by spherical particles with an average diameter of 55 nm (Fig. 8A) which are aggregated into chains, due to magnetic and electrostatic interactions between them [53]. The individual particles present a core-shell structure (Fig. 8B) in which, according to the EDS analysis (data not shown for the sake of clarity of the figures) and in agreement with other authors [54], the external shell is composed for iron and oxygen and surrounds the core of metallic iron. The core-shell structure became progressively more diffuse after the use of the nZVI in consecutive reactions (Fig. 8D, E and F) until almost disappear. The LEED analysis shows that the new structure of the core is composed of wüstite (FeO), despite this was not detected by XRD. The change of the

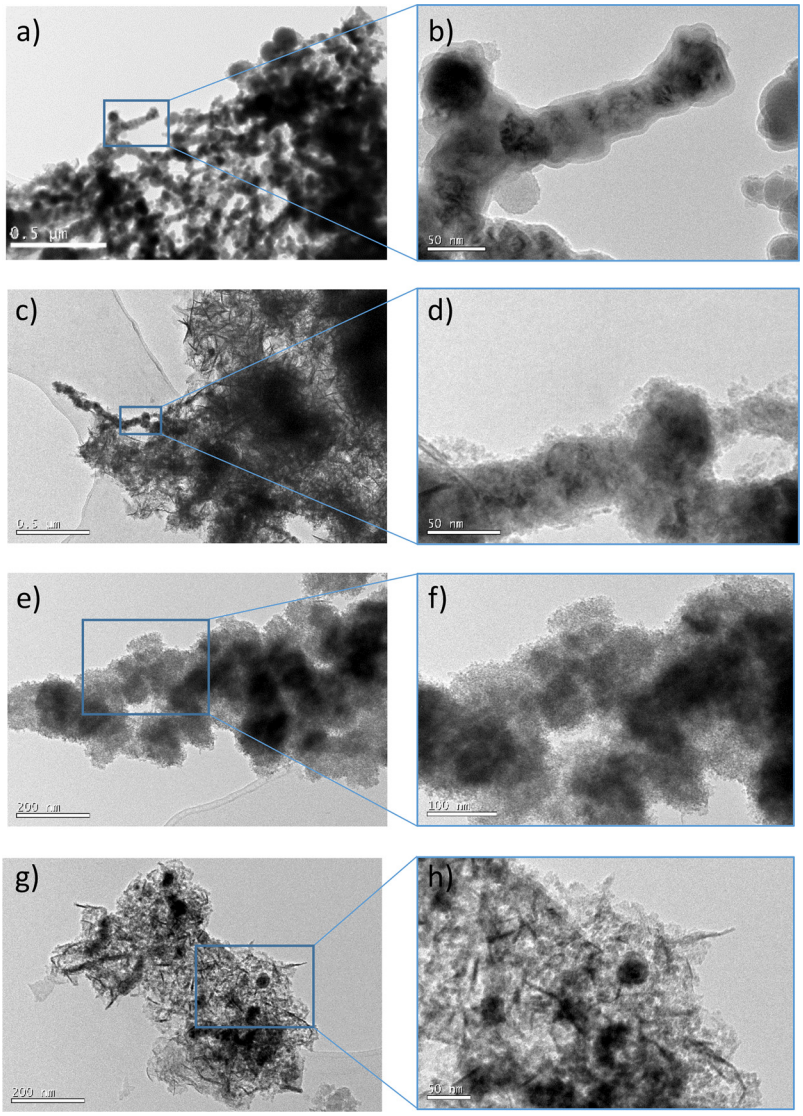

Fig. 8. Bright field TEM micrograph of nZVI: a) and b) fresh nZVI; c) and d) recovered nZVI particles after the first use in reaction; e) and f) recovered nZVI particles after second use in reaction; g) and h) recovered nZVI particles after third use in reaction.

structure of nZVI can be explained by a plausible mechanism of dissolution–precipitation of the iron. In turn, throughout the consecutive reactions, flaky structures are gradually formed, being predominant in the nZVI material recovered after the third reaction (Fig. 8G and H). The results are in agreement with the XRD analysis, as flaky structures are associated to the presence of lepidocrocite (γ-FeOOH), probably formed by re-precipitation of dissolved iron [52]. The EDS analysis revealed that the new structure was composed by iron and oxygen, however in this case, it was not possible to identify the crystalline phase by LEED.

4. Conclusions

This investigation proved the inactivation of *E.coli* and *Enterococcus sp.* in simulated wastewater samples by sulfate radicals. Different iron species in homogeneous ($FeSO_4$; Fe(III)-citrate) and heterogeneous phase (Fe_2O_3; nZVI) were tested as activator of PMS and PS in presence of UV-A radiation. It was proved that PMS always reached better bacteria inactivation efficiencies than PS, what can be explained by the direct generation not only of sulfate radicals but also hydroxyl radicals by the fission of PMS molecule. By contrast, for PS hydroxyl radicals only can be generated by photo-reduction of Fe(III).

The use of diverse iron species showed different efficiencies in the inactivation of both bacteria. A 5-log abatement of *E. coli*, reaching the detection limit could be attained within 2–15 min by activation of PMS and PS with all the iron sources evaluated. By contrast, *Enterococcus sp.* could not be removed over 90 min beyond a 3.50-log decrease, in any of the experimental conditions.

The use of Fe(III) as activator had a beneficial influence on the inactivation kinetics for *Enterococcus sp.* not observed, on the contrary, for *E. coli*. In comparison to the 1.9-log decrease attained with the use of homogeneous Fe(II) after 90 min, the highest *Enterococcus sp.* inactivation (3.50-log in 90 min) was reached through the use of Fe(III)-citrate. The results can be explained considering that the photolysis of Fe(III)-citrate generates additional oxidative species such as hydrogen peroxide (H_2O_2) and superoxide radical ($O_2^{\bullet-}$), that contribute to bacteria inactivation. The beneficial effect of these reactions would not be appreciable in the case of *E.coli* because of the much faster removal of the bacteria attained with homogeneous Fe(II) and PMS or PS.

The use of nZVI as a heterogeneous source of iron showed promising results in terms of inactivation of both bacteria, in combination with PMS or PS and UV-A radiation. *E.coli* was totally reduced (5-log) after 5 min of treatment with PMS, and 15 min with PS, whereas a 2-log decrease in *Enterococcus sp. was* achieved in presence of PMS. The

possibility of recovering and re-use this material would reduce the operating costs of the treatment. Nevertheless, the first approach showed that oxidants and UV-A radiation oxidized the nZVI particles changing its chemical structure and therefore reducing the efficiency of the catalyst in consecutive reactions.

Finally, the differences in the efficiency of the oxidant/iron/UVA treatments observed between the studied bacteria can be explained as a direct consequence of the different bacterial structure. In agreement with previous reports [21] Gram-positive bacteria *Enterococcus sp.* was more resistant to oxidative treatments under irradiation than Gram-negative bacteria *E.coli*.

Acknowledgements

"This Special Issue is dedicated to honor the retirement of Prof. César Pulgarin at the Swiss Federal Institute of Technology (EPFL, Switzerland), a key figure in the area of Catalytic Advanced Oxidation Processes". Besides J. Rodríguez-Chueca acknowledges Universidad Politécnica de Madrid for the support through the research project VJIDOCUPM18JJRC, and M.J. López-Muñoz and J.M. Raez acknowledge the financial support from the Spanish Ministerio de Economía y Competitividad and Fondo Europeo de Desarrollo Regional through the research project CTM2015-69246-R (MINECO/FEDER).

References

[1] E. Metzger, B. Owens, P. Reig, W.H. Wen, R. Young, World Water Resour. (2016) ISBN 978-1-56973-883-2.
[2] G. Ferro, A. Fiorentino, M. Castro Alférez, M.I. Polo-López, L. Rizzo, P. Fernández-Ibáñez, Appl. Catal. B Environ. 178 (2015) 65–73.
[3] J. Rodríguez-Chueca, E. Laski, C. García-Cañibano, M.J. Martín de Vidales, Á. Encinas, B. Kuch, J. Marugán, Sci. Total Environ. 630 (2018) 1216–1225.
[4] S.B. Hammouda, F. Zhao, Z. Safaei, D.L. Ramasamy, B. Doshi, M. Sillanpää, Appl. Catal. B Environ. 233 (2018) 99–111.
[5] A. Rastogi, S.R. Al-Abed, D.D. Dionysiou, Appl. Catal. B Environ. 85 (3–4) (2009) 171–179.
[6] L. Ismail, C. Ferronato, L. Fine, F. Jaber, J.M. Chovelon, Appl. Catal. B Environ. 201 (2017) 573–581.
[7] H.V. Lutze, J. Brekenfeld, S. Naumov, C. von Sonntag, T.C. Schmidt, Water Res. 129 (2018) 509–519.
[8] J. Rodríguez-Chueca, T. Silva, J.R. Fernandes, M.S. Lucas, G. Li Puma, J.A. Peres, A. Sampaio, Water Res. 123 (2017) 113–123.
[9] J. Rodríguez-Chueca, S.I. Moreira, M.S. Lucas, J.R. Fernandes, P.B. Tavares, A. Sampaio, J.A. Peres, J. Clean. Prod. 149 (2017) 805–817.
[10] M. Marjanovic, S. Giannakis, D. Grandjean, L.F. de Alencastro, C. Pulgarin, Water Res. 140 (2018) 220–231.
[11] A. Bianco, M.I. Polo – López, P. Fernández – Ibáñez, M. Brigante, G. Mailhot, Water Res. 118 (2017) 249–260.
[12] J. Wang, S. Wang, Chem. Eng. J. 334 (2018) 1502–1517.
[13] P. Neta, R.E. Huie, J. Phys. Chem. Ref. Data 17 (3) (1988) 1027–1284.
[14] P. Wardman, J. Phys. Chem. Ref. Data 18 (4) (1989) 1637–1755.
[15] H. Herrmann, Phys. Chem. Chem. Phys. 9 (2007) 3935–3964.
[16] S. Verma, S. Nakamura, M. Sillanpää, Chem. Eng. J. 284 (2016) 122–129.
[17] G.P. Anipsitakis, D.D. Dionysiou, Environ. Sci. Technol. 38 (2004) 3705–3712.
[18] J. Rodríguez-Chueca, C. Amor, T. Silva, D.D. Dionysiou, G. Li Puma, M.S. Lucas, J.A. Peres, Chem. Eng. J. 310 (2) (2017) 473–483.
[19] P. Hu, M. Long, Appl. Catal. B Environ. 181 (2016) 103–117.
[20] X. Zeng, J. Chen, R. Qu, M. Feng, Z. Wang, Chem. Eng. J. 319 (2017) 98–107.
[21] J. Rodríguez-Chueca, M. Polo-López, R. Mosteo, M. Ormad, P. Fernandez-Ibáñez, Appl. Catal. B Environ. 150 (2014) 619–629.
[22] OECD, Guidelines for testing of chemicals, Simulation Test-Aerobic Sewage Treatment 303A, (1999).
[23] S.M. Ponder, J.G. Darab, T.E. Mallouk, Environ. Sci. Technol. 34 (2000) 2564–2569.
[24] APHA, Standard Methods for the Examination of Water and Waste Water, 21st edn., American Public Health Association, Washington DC (United States of America), 2005.
[25] J. Rodríguez-Chueca, C. García-Cañibano, R.-J. Lepistö, Á. Encinas, J. Pellinen, J. Marugán, J. Hazard. Mater. (2018), https://doi.org/10.1016/j.jhazmat.2018.04.044.
[26] P. Sun, C. Tyree, C.H. Huang, Environ. Sci. Technol. 50 (2016) 4448–4458.
[27] J.J. Pignatello, E. Oliveros, A. MacKay, Crit. Rev. Environ. Sci. Technol. 36 (1) (2006) 1–84.
[28] P.K. Dutta, S.O. Pehkonen, V.K. Sharma, A.K. Ray, Environ. Sci. Technol. 39 (6) (2005) 1827–1834.
[29] M. Owoseni, A. Okoh, Int. Biodeterior. Biodegrad. 120 (2017) 216–223.
[30] Guidelines for drinking-water quality, World Health Org. 1 (2006) 1–597 (Geneve, Switzerland).
[31] J. Rodríguez-Chueca, M.P. Ormad, R. Mosteo, J.L. Ovelleiro, Chem. Eng. Sci. 138 (2015) 730–740.
[32] J. Moreno-Andrés, L. Romero-Martínez, A. Acevedo-Merino, E. Nebot, Chem. Eng. J. 283 (2016) 1339–1348.
[33] M. Figueredo-Fernández, S. Gutiérrez-Alfaro, A. Acevedo-Merino, M.A. Manzano, Sol. Energy 158 (2017) 303–310.
[34] H.B. Abrahamson, A.B. Rezvani, J.G. Brushmiller, Inorg. Chim. Acta Rev. 226 (1-2) (1994) 117–127.
[35] N. Quici, M.E. Morgada, R.T. Gettar, M. Bolte, M.I. Litter, Appl. Catal. B Environ. 71 (3–4) (2007) 117–124.
[36] C. Weller, S. Horn, H. Herrmann, J. Photochem. Photobiol. 268 (2013) 24–36.
[37] N. Seraghni, S. Belattar, Y. Mameri, N. Debbache, T. Sehili, Int. J. Photoenergy (2012) 630425.
[38] L. Luo, D. Wu, D. Dai, Z. Yang, L. Chen, Q. Liu, J. He, Y. Yao, Appl. Catal. B: Environ. 205 (2017) 404–411.
[39] L. Ling, D. Zhang, C. Fan, C. Shang, Water Res. 124 (2017) 446–453.
[40] L. Ling, D. Zhang, J. Fang, C. Fan, C. Shang, Chemosphere 184 (2017) 417–428.
[41] C. Zhang, L. Wang, F. Wu, N. Deng, Environ. Sci. Pollut. Res. 13 (3) (2005) 156–160.
[42] F. Ghanbari, M. Moradi, Chem. Eng. J. 310 (2017) 41–62.
[43] G. Vilardi, J. Rodríguez-Rodríguez, J.M. Ochando-Pulido, N. Verdone, A. Martinez-Ferez, L. Di Palma, Process Saf. Environ. 117 (2018) 629–638.
[44] G. Li, Q. Xu, X. Jin, R. Li, R. Dharmarajan, Z. Chen, Sep. Purif. Technol. 197 (2018) 401–406.
[45] Y. Liu, S. Zha, D. Rajarathnam, Z. Chen, Sep. Purif. Technol. 188 (2017) 548–552.
[46] Y.G. Kang, H. Yoon, W. Lee, E. Kim, Y.S. Chang, Chem. Eng. J. 334 (2018) 2511–2519.
[47] Y. Gao, N. Gao, W. Wang, S. Kang, J. Xu, H. Xiang, D. Yin, Ultrason. Sonochem. (2018), https://doi.org/10.1016/j.ultsonch.2018.07.001.
[48] H. Dong, Q. He, G. Zeng, L. Tang, L. Zhang, Y. Xie, Y. Zeng, F. Zhao, Chem. Eng. J. 316 (2017) 410–418.
[49] F.M. Alizadeh, T. Ali, B.G.R. Nabi, A. Behnoush, J. Environ. Eng. 139 (2013) 966–974.
[50] M.E. Morgada, I.K. Levy, V. Salomone, S.S. Farias, G. Lopez, M.I. Litter, Catal. Today 143 (2009) 261–268.
[51] S. Yousefzadeh, A.R. Matin, E. Ahmadi, Z. Sabeti, M. Alimohammadi, H. Aslani, R. Nabizadeh, Food Chem. Toxicol. 114 (2018) 334–345.
[52] A. Liu, J. Liu, J. Han, W. Zhang, J. Hazard. Mater. 322 (A (2017) 129–135.
[53] Ç. Üzüm, T. Shahwan, A.E. Eroğlu, I. Lieberwirth, T.B. Scott, K.R. Hallam, Chem. Eng. J. 144 (2) (2008) 213–220.
[54] W. Yan, A.A. Herzing, C. Kiely, W. Zhang, J. Contam. Hydrol. 118 (3-4) (2010) 96–104.